

## Supporting Information

### Factors Influencing Preferential Anion Interactions during Solvation of Multivalent Cations in Ethereal Solvents

Kee Sung Han<sup>†,§,†</sup>, Nathan T. Hahn<sup>‡,§,†</sup>, Kevin R. Zavadil<sup>‡,§</sup>, Nicholas R. Jaegers<sup>†</sup>, Ying Chen<sup>†,§</sup>, Jian Zhi Hu<sup>†,§</sup>, Vijayakumar Murugesan<sup>\*†,§</sup>, and Karl T. Mueller<sup>\*†,§</sup>

<sup>†</sup>Pacific Northwest National Laboratory, Richland, Washington 99352, United States

<sup>‡</sup>Sandia National Laboratories, Albuquerque, New Mexico 87123, United States

<sup>§</sup>Joint Center for Energy Storage Research (JCESR), Lemont, Illinois 60439, United States.

**Table S1. Diffusion coefficients of TFSI anions and solvent molecules (G1, G3, THF and 2-MeTHF) across the tested series of electrolytes. Actual salt concentrations are summarized in Table 1.**

Samples	Diffusion coefficients (m <sup>2</sup> /s)*			
	Low concentration		High Concentration	
	Anion	Solvent	Anion	Solvent
Zn(TFSI)2/G1	3.0 × 10 <sup>-10</sup>	1.5 × 10 <sup>-9</sup>	2.7 × 10 <sup>-10</sup>	1.0 × 10 <sup>-9</sup>
Zn(TFSI)2/G3	1.4 × 10 <sup>-10</sup>	4.3 × 10 <sup>-10</sup>	8.3 × 10 <sup>-11</sup>	1.7 × 10 <sup>-10</sup>
Zn(TFSI)2/THF	2.2 × 10 <sup>-9</sup>	3.1 × 10 <sup>-9</sup>	1.0 × 10 <sup>-9</sup>	3.1 × 10 <sup>-9</sup>
Zn(TFSI)2/2-MeTHF	7.8 × 10 <sup>-10</sup>	2.2 × 10 <sup>-9</sup>	4.0 × 10 <sup>-10</sup>	1.3 × 10 <sup>-9</sup>
Ca(TFSI)2/G1	7.4 × 10 <sup>-10</sup>	2.6 × 10 <sup>-9</sup>	4.4 × 10 <sup>-10</sup>	1.6 × 10 <sup>-9</sup>
Ca(TFSI)2/G3	1.3 × 10 <sup>-10</sup>	4.3 × 10 <sup>-10</sup>	7.8 × 10 <sup>-11</sup>	1.8 × 10 <sup>-10</sup>
Ca(TFSI)2/THF	7.3 × 10 <sup>-10</sup>	2.3 × 10 <sup>-9</sup>	3.7 × 10 <sup>-10</sup>	1.4 × 10 <sup>-9</sup>
Ca(TFSI)2/2-MeTHF	1.0 × 10 <sup>-9</sup>	2.6 × 10 <sup>-9</sup>	5.2 × 10 <sup>-10</sup>	1.3 × 10 <sup>-9</sup>

\*The errors in fitting the PFG-echo profiles are less than ±3% of each reported diffusion coefficient.

#### Estimation of the Degree of SSIP Formation from Raman Spectroscopy.

Raman spectroscopy was performed on solutions sealed in glass vials using a Witec Confocal Raman Microscope equipped with a 532 nm laser. Fitting of the TFSI breathing mode region (~740 cm<sup>-1</sup>) was performed using three discrete, semi-constrained Lorentzian/Gaussian components (one for uncoordinated TFSI, two for bound TFSI), in accordance with established methods (Giffin, G. A., *et al*, *J. Phys. Chem. C* **2014**, 118, (19), 9966-9973 and Watkins, T., *et al*, *J. Phys. Chem. B* **2015**, 119, (23), 7003-7014).

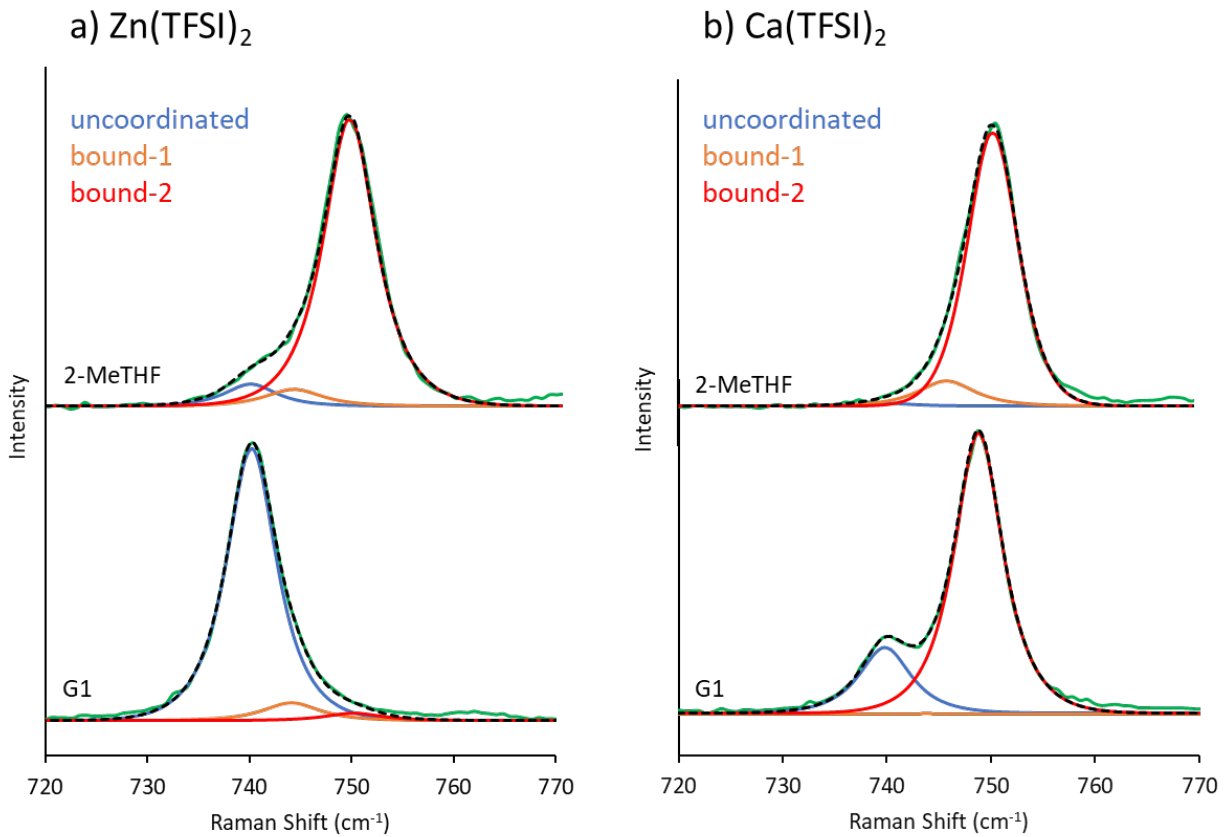


**Figure S1.** Example deconvoluted Raman spectra of the TFSI breathing mode region in  $\sim 0.5$  M solutions of a)  $\text{Zn}(\text{TFSI})_2$  and b)  $\text{Ca}(\text{TFSI})_2$  in 2-MeTHF and G1. The experimental spectrum is depicted as a solid green line while the deconvoluted fit is depicted as a dashed black line. The uncoordinated TFSI component (blue line) has a frequency of  $\sim 740$   $\text{cm}^{-1}$  and its integrated intensity relative to the total integrated intensity of this region is used to quantify the percentage of uncoordinated TFSI, as shown in main text Figure 2c.

#### Dielectric Constant Measurements from Dielectric Relaxation Spectroscopy.

Broadband DRS measurements (from 0.5 to 26.5 GHz) were conducted using a three-point calibration of air, water, and tetrahydrofuran. Subsequent solution measurements were made across a range of salt concentrations. In each case the real ( $\varepsilon'$ ) and imaginary ( $\varepsilon''$ ) components of the complex permittivity spectra are extracted and fitted simultaneously according to equation 1 (Buchner, R. *et al*, *Annu. Rep. Prog. Chem., Sect. C: Phys. Chem.*, **2001**, 97, 349-382):

$$\varepsilon(\nu) = \varepsilon_\infty + \sum_{j=1}^n \varepsilon_j \left[ 1 - (i2\pi\nu\tau_j)^{1-\alpha_j} \right]^{-1} \quad (1)$$

Here, the frequency-dependent permittivity ( $\varepsilon$ ) is deconvoluted into the high frequency intramolecular permittivity ( $\varepsilon_\infty$ ) and  $n$  distinct Debye ( $\alpha = 0$ ) or Cole-Cole ( $\alpha \neq 0$ ) relaxation processes each having a characteristic permittivity amplitude ( $\varepsilon$ ) and time constant ( $\tau$ ). In addition to these three parameters, the ionic conductivity (which influences  $\varepsilon''$  but not  $\varepsilon'$ ) was treated as an adjustable parameter during fitting. The lower frequency bound used for fitting was adjusted to 0.7 GHz in some cases to account for errors associated with high ionic conductivity. Each relaxation represents the re-orientations of dipoles in solution, occurring primarily within the microwave frequency range. These correspond to solvent molecules as well

as dipolar ion clusters such as contact ion pairs (CIPs) or solvent-separated ion pairs (SSIPs). While CIPs can generally be detected by Raman spectroscopy, DRS is highly sensitive to SSIPs as these species have very large dipole moments. Typically, three relaxation processes were found to yield accurate fits to the measured data, and extrapolation of these fits to  $\nu = 0$  thus yields a reasonable estimation of the dielectric constant. Based on the neat solvent data, the fastest relaxation is ascribed to free solvent while slower relaxations are related to salt species. In this work, the primary information sought is the change in solution dielectric constant as a function of salt concentration as a result of the ion pair species. Select spectra as well as the extracted dielectric constants are plotted in main text Figure 4. The fitting parameters extracted from these spectra are shown in Table S2, and example deconvolutions of the  $\text{Ca}(\text{TFSI})_2/\text{G1}$  electrolytes are shown in Figure S2. Measurements of the neat solvents yielded dielectric constants very similar to the literature values shown in Table 2.

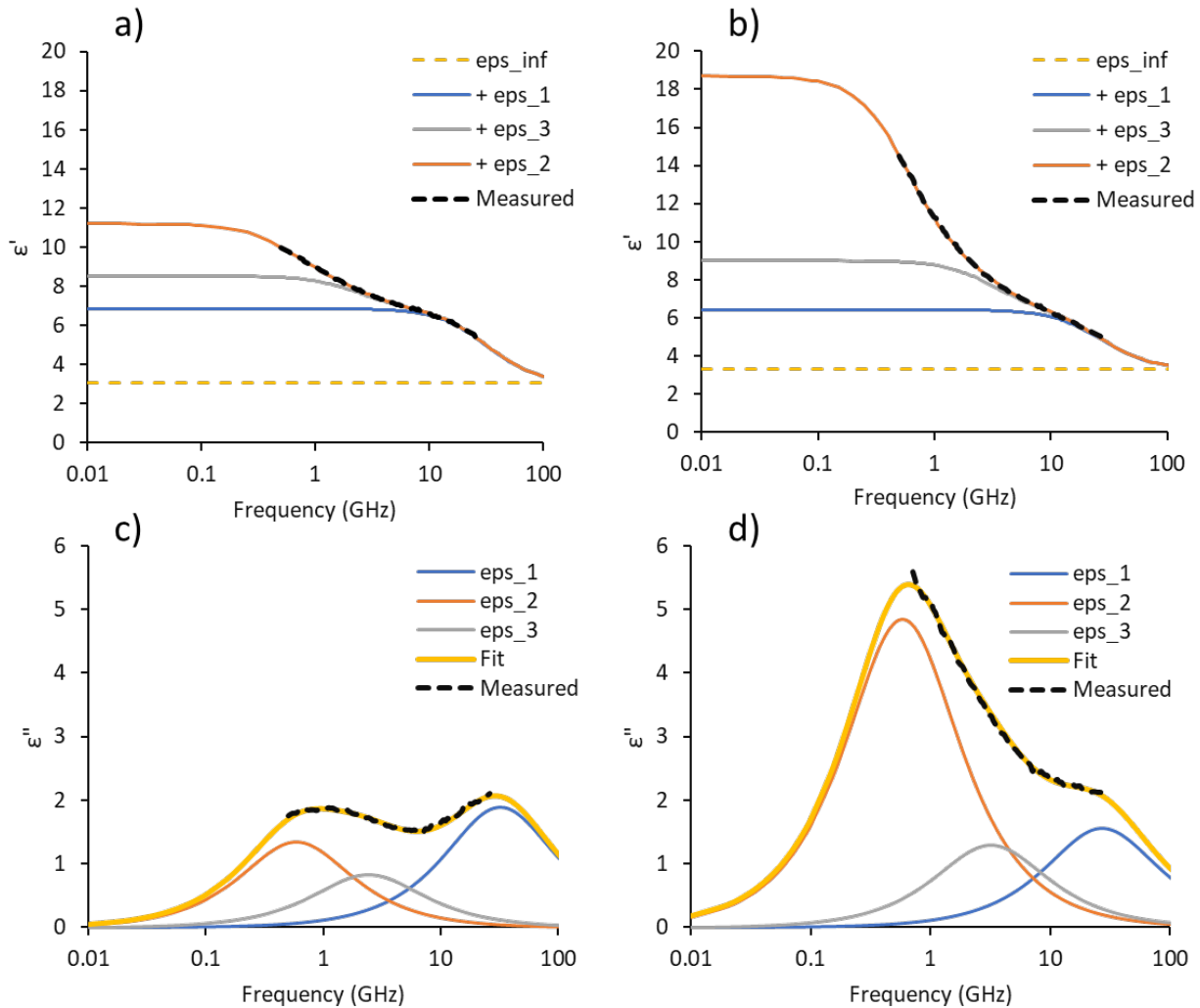


**Figure S2.** Example deconvoluted DRS spectra for  $\text{Ca}(\text{TFSI})_2/\text{G1}$  solutions at 0.1 M (a,c) and 0.4 M (b,d) salt concentrations. These spectra depict the contributions of each relaxation component to the real and imaginary spectra. This comparison clearly illustrates how the low frequency salt dipoles, i.e. ion pairs, contribute dramatically to the overall solution permittivity.

**Table S2. DRS measurement parameters for select Zn(TFSI)<sub>2</sub> and Ca(TFSI)<sub>2</sub> electrolytes at 21°C obtained from a fit incorporating three Debye ( $\alpha = 0$ ) and/or Cole-Cole relaxations.**

<b>Sample</b>	<i>Solvent Relaxations</i>				<i>Salt Relaxations</i>				
	$\varepsilon_\infty$	$\varepsilon_1$	$\tau_1^a$	$\alpha_1$	$\varepsilon_2$	$\tau_2^a$	$\varepsilon_3$	$\tau_3^a$	$\varepsilon_r$
Neat G1	2.91	4.13	4.6	0	-	-	-	-	<b>7.05</b>
Neat G3	2.94	4.64	11.7	0.12	-	-	-	-	<b>7.59</b>
0.035M ZnTFSI <sub>2</sub> /G1	2.89	4.13	4.5	0	1.36	314	0.78	52	<b>9.16</b>
0.5M ZnTFSI <sub>2</sub> /G1	3.59	3.30	6.3	0	6.18	272	3.28	40	<b>16.36</b>
0.1M Ca(TFSI) <sub>2</sub> /G1	3.07	3.79	5.0	0	2.93	272	1.10	66	<b>11.19</b>
0.4M Ca(TFSI) <sub>2</sub> /G1	3.31	3.12	5.9	0	9.69	274	2.57	50	<b>18.69</b>
0.1M Ca(TFSI) <sub>2</sub> /G3	2.98	4.11	10.4	0.12 <sup>b</sup>	4.17	461	1.11	45	<b>12.37</b>
0.5M Ca(TFSI) <sub>2</sub> /G3	3.44	3.12	9.8	0.12 <sup>b</sup>	5.81	370	2.57	49	<b>14.95</b>

<sup>a</sup>Relaxation time constants given in ps

<sup>b</sup>Fixed parameter based on neat solvent value